

Performance of the first-light adaptive optics system of LBT by means of CAOS simulations

Marcel Carbillot^a, Christophe Vérinaud^a, Simone Esposito^a, Armando Riccardi^a,
Alfio Puglisi^a, Bruno Femenía^b, Luca Fini^a,

^aINAF – Osservatorio Astrofisico di Arcetri, largo E. Fermi 5, 50125 Firenze, Italy

^bGranTeCan, vía Láctea s/n (IAC), 38200 La Laguna, Spain

ABSTRACT

This presentation reports the numerical simulations we have done in order to evaluate the performance of the first-light AO system of LBT. The simulation tool used for this purpose is the Software Package CAOS, applicable for a wide range of AO systems and for which a brief recall of the main features is made. The whole process of atmospheric propagation of light, wavefront sensing (using a complete model of the pyramid wavefront sensor), wavefront reconstruction (using the LBT 672 adaptive secondary mirror modes), and closing of the loop, is simulated. The results are given in terms of obtained Strehl ratios in J-, H-, and K-band. Estimation of the resulting sky-coverage in K-band for different regions of the sky are also expressed. A comparison with the performance that would be obtained by using a Shack-Hartmann sensor is presented, confirming the gain achievable with the pyramid sensor.

Keywords: Large Binocular Telescope, first-light adaptive optics system, pyramid wavefront sensor, numerical simulations

1. INTRODUCTION

The first-light adaptive optics (AO) system of the Large Binocular Telescope (LBT)⁹ is foreseen to operate in summer 2004. It is a part of the acquisition, guiding and wavefront sensing (AGW) unit of LBT.¹³ A complete description of the system is given in Esposito et al.,⁷ while the LBT 672 adaptive secondary mirror features are described in Riccardi et al.¹² In this paper we focus on the numerical study we have made in order to evaluate the performance of our system.

Involving many physical processes, each corresponding to a large number of parameters, the simulation results presented here permit to characterize the ensemble of choices made for the design of our system. They also give a number of useful indications on the system behaviour when on-sky operation will be made, and on the optimization of a series of free parameters. The results found are expressed in terms of obtained Strehl ratio in J-, H-, and K-band (and then in terms of sky coverage), and include a comparison with a Shack-Hartmann-based system.

The paper is organised as follows. In Sec. 2 we recall the main features of the numerical tool used for this purpose, CAOS.² Then in Sec. 3 we expose the main parameters of the problem and describe the simulation procedure we have followed, giving as well some example of our exploring of the hyper-space of parameters considered here. Finally the obtained performance in terms of Strehl ratios in the imaging bands J, H, and K are given in Sec. 4. It also include a comparison with the results that would be obtained using a Shack-Hartmann wavefront sensor, and the estimated resulting performance in terms of sky coverage. We then give our conclusions in Sec. 5, together with a couple of additional remarks concerning the use of low-RON detectors for wavefront sensing in one hand, and the issue of dynamical modulation of the pyramid in the other hand.

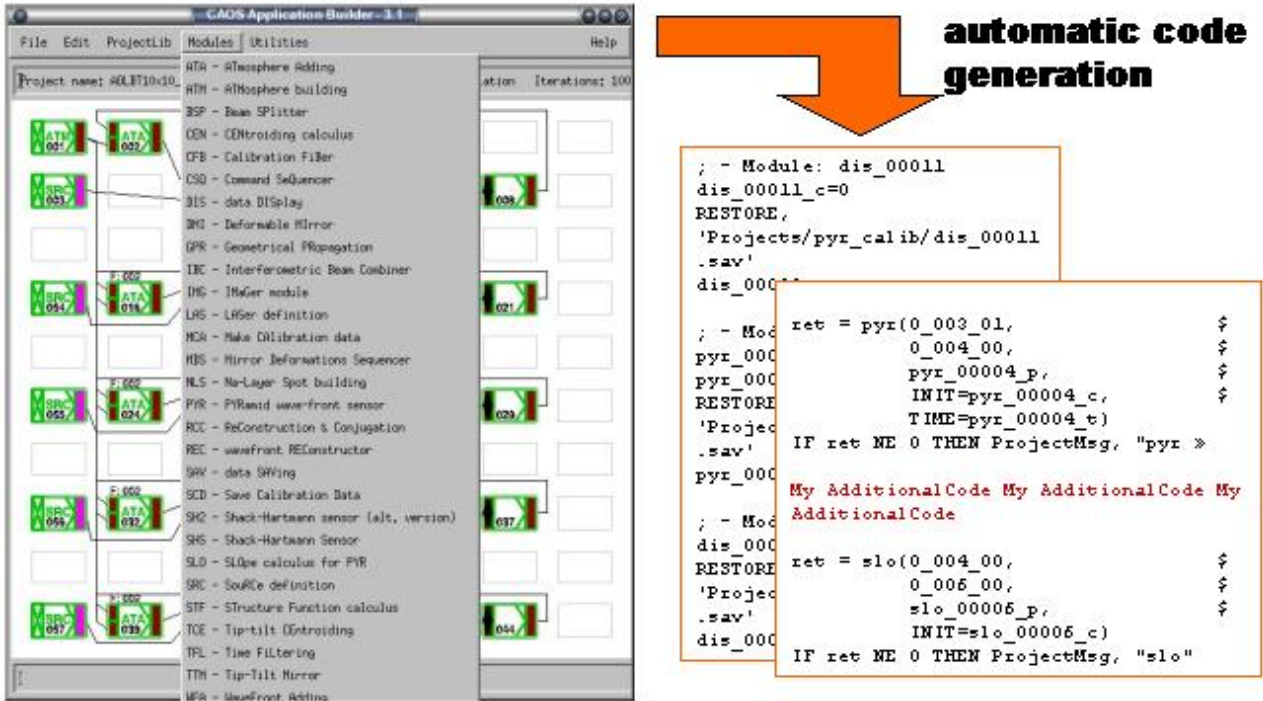


Figure 1. Layout of the CAOS Application Builder graphical programming environment, showing the list of modules taken from the Software Package CAOS and an example of project designed for the simulation of the first-light AO system of LBT. The capability of generating automatically the code resulting from the designed simulation is also illustrated.

2. THE NUMERICAL TOOL USED: CAOS

The simulation tool used for the simulations presented here is CAOS (Code for Adaptive Optics Systems). It is essentially a set of modules – the Software Package CAOS^{2,14} – designed to be used within a graphical programming environment – the CAOS Application Builder⁸ where the data flow and the parameters of each module can be set. We are here interested in AO simulations, but it is worthy to notice that any kind of other applications can be easily implemented within this environment, as for example the Software Package AIRY^{3,4} dedicated to multiple deconvolution of interferometric images. Another important point is that it is very easy to implement new modules within a given Software Package, by simply adapting a given already existing IDL code within the templates given along with the CAOS Application Builder source. The programming environment also provides closing-loop capability, essential for AO simulations.

The structure of our numerical tool being modular, each physical elementary process of a given simulation is modeled within a specific module – like, in the AO case, the turbulence in each atmospheric layer, the propagation of the light from a source to the observing telescope and through the turbulent layers, the wavefront sensing, the wavefront reconstruction, time-filtering of the resulting deformable mirror commands, the wavefront correction, etc. Taking advantage from the CAOS Application Builder, a simulation can be built putting and connecting together the required occurrences of the desired modules, respecting the only logical constraint given by their formalized type of input/output. Each module comes with an individual GUI in order to set its own physical and numerical parameters, during the design step or independently in a later moment. The whole structure of a simulation can be saved as a “project” that can be restored for later modifications and/or parameters upgrading. The IDL code, corresponding to the designed simulation, is written down during the saving of a project, and it can possibly be modified “by hand” in order to be completed with some additional task not provided by strictly using the Software Package CAOS. Figure 1 shows a typical simulation design

Correspondance e-mail: marcel@arcetri.astro.it

obtained with the CAOS Application Builder, together with the list of modules available from the Software Package CAOS, and a sample of automatically generated code.

More detailed informations about this numerical simulation tool and the already developed associated packages can be found from the dedicated web-site www.arcetri.astro.it/caos.

3. MAIN PARAMETERS ASSUMED AND SIMULATION PROCEDURE ADOPTED

Our goal is to evaluate the performance of the first-light AO system for LBT by means of CAOS simulations. A wide range of situations have been simulated, in which we have played with the different parameters in order to find some kind of optimum values for the configuration, the integration time (both implying a given RON), the pyramid modulation, the number of LBT672 mechanical modes to reconstruct, all together in function of the magnitude of the guide star which photons feed the AO system for wavefront sensing and reconstruction. The parameters used to obtain the simulation results reported in the following are reported here below:

- Turbulent atmosphere:
 - two layers of wind velocity 15 m/s.
 - Fried parameter r_0 (@500 nm)=0.15 cm (that corresponds to $\lambda/r_0 \simeq 0.67$ arcsec).
 - wavefront outer scale $L_0=40$ m.
 - resulting seeing $\epsilon \simeq 0.5$ arcsec.
- Guide star:
 - K5 spectral type.
 - R-magnitude: from 7.6 to 17.1.
- Telescope:
 - effective diameter $D = 8.25$ m.
 - obscuration ratio $\epsilon = 0.11$.
- Pyramid wavefront sensor:
 - configurations: 10×10 , 15×15 , and 30×30 equivalent subapertures (i.e. CCD binning of 3×3 , 2×2 , and 1×1 , respectively).
 - exposure time: from 1 ms to 10 ms (all configurations).
 - RON: from 3.5 to 8.4 e- RMS (depending upon both previous parameters).
 - modulation: up to $\pm 8\lambda/D$.
 - telescope+optics transmission $\tau = 0.9^3 * 0.7$.
 - spectral band: $750 \text{ nm} \pm 150 \text{ nm}$ (i.e. roughly R and a part of I).
 - average quantum efficiency over considered band: 0.81.
- Wavefront reconstruction: up to 671 LBT 672 mechanical modes reconstructed (the lack one being the piston).
- Imaging device:
 - pixel size $\Delta x = 10$ mas (all bands),
 - bands (central wavelength): J (1250 nm), H (1650 nm), and K (2200 nm).

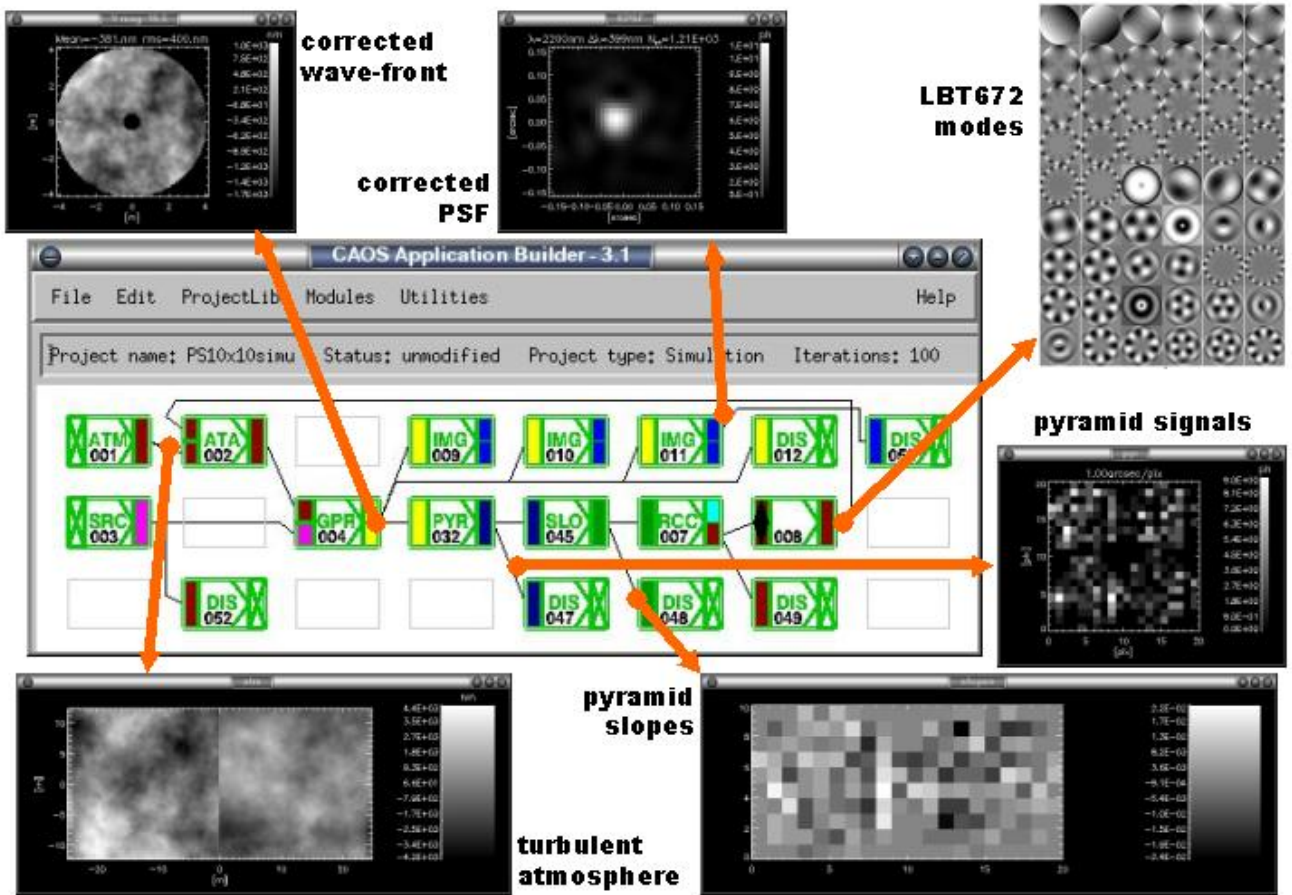


Figure 2. Simulation procedure followed.

Figure 2 shows the simulation procedure followed within the CAOS Application Builder and using the modules of the Software Package CAOS. The output of the module ATM simulating the atmosphere (made of two moving turbulent layers) is sent to module ATA that mimic the correction due to the deformable mirror (the adaptive secondary mirror in our case) into a "correction" layer (here conjugated to the ground). The resulting corrected wavefront is then computed by the module GPR that basically propagates the light between the guide star defined within module SRC and the telescope which characteristics are set by using the GUI of GPR. The resulting corrected wavefront is then taken into account by module PYR that simulates the behavior of the pyramid wavefront sensor, and the resulting signals (see figure) are then sent to a slope calculator (SLO) that compute the slopes corresponding to each subaperture of the pyramid wavefront sensor, before sending the result to the wavefront reconstructor RCC that reconstruct the wavefront by using the LBT 672 computed modes. The loop is then closed by a special module (part of the Application Builder) that send the result to previously evocated module ATA. During each step of the simulation the resulting PSFs are computed within the occurrences of module IMG in J-, H-, and K-band, and the different quantities of interest (the atmosphere, the corrected wavefront, the corrected PSFs, the pyramid signals and slopes, the correction) can be displayed and/or saved by using some additionnal utility modules.

A quite noticeable remark is that each process is simulated as close as possible to the real-life situation. For example the pyramid sensor, in which diffraction effects play a certain role on the performance of the system, is simulated following the following scheme: the electric field in the image plane is masked for each facet of the pyramid, resulting after diffraction computation in the four-pupil image of Fig. 2. The pyramid can also be simulated, still within the Software Package CAOS, by simulating the pyramid as a phase mask, as described

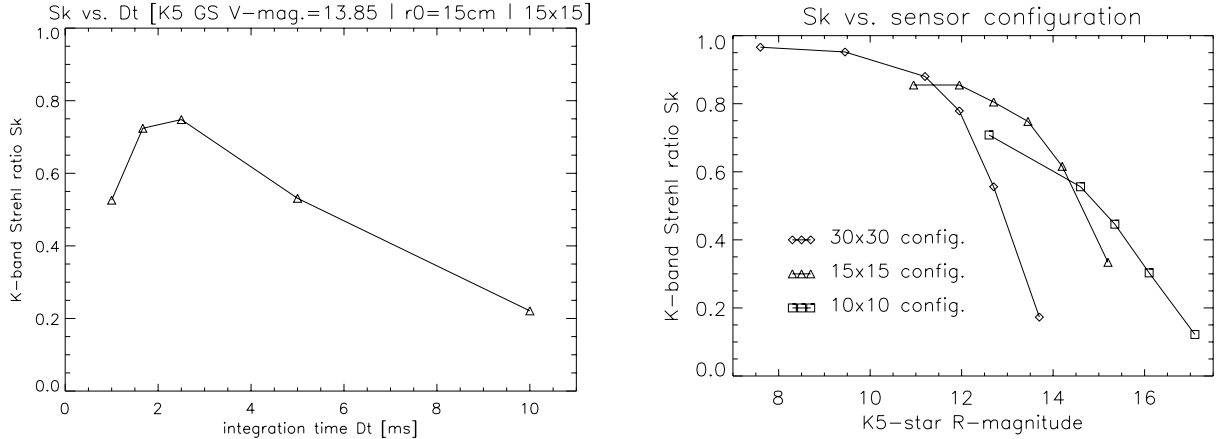


Figure 3. Left: optimization of the integration time (and subsequent RON) for the configuration 15×15 for one case of GS-magnitude, and number of corrected modes, in terms of K-Strehl performance. Right: optimization of the configuration for the different cases of magnitude, number of corrected modes, and integration time.

in V erinaud et al.¹⁵

We have designed this typical simulation for the different configurations of the wavefront sensor and run it for a wide range of parameters defining each consecutive process of the whole simulation, exploring so the hyper-space of parameters as extensively as possible. Figure 3 shows two examples of search for optimum within the hyper-space of free parameters given by the present problem. The parameters for which this work has been performed are: the integration time (and hence the corresponding RON), the number of LBT 672 modes corrected, the pyramid modulation, the gain of the closed loop, and the sensor configuration.

4. RESULTING PERFORMANCE

Figure 4 shows the best values found for the J-, H-, K-Strehl ratios obtained in function of the R-magnitude of a K5 spectral type guide star. The parameters corresponding to each point are also reported.

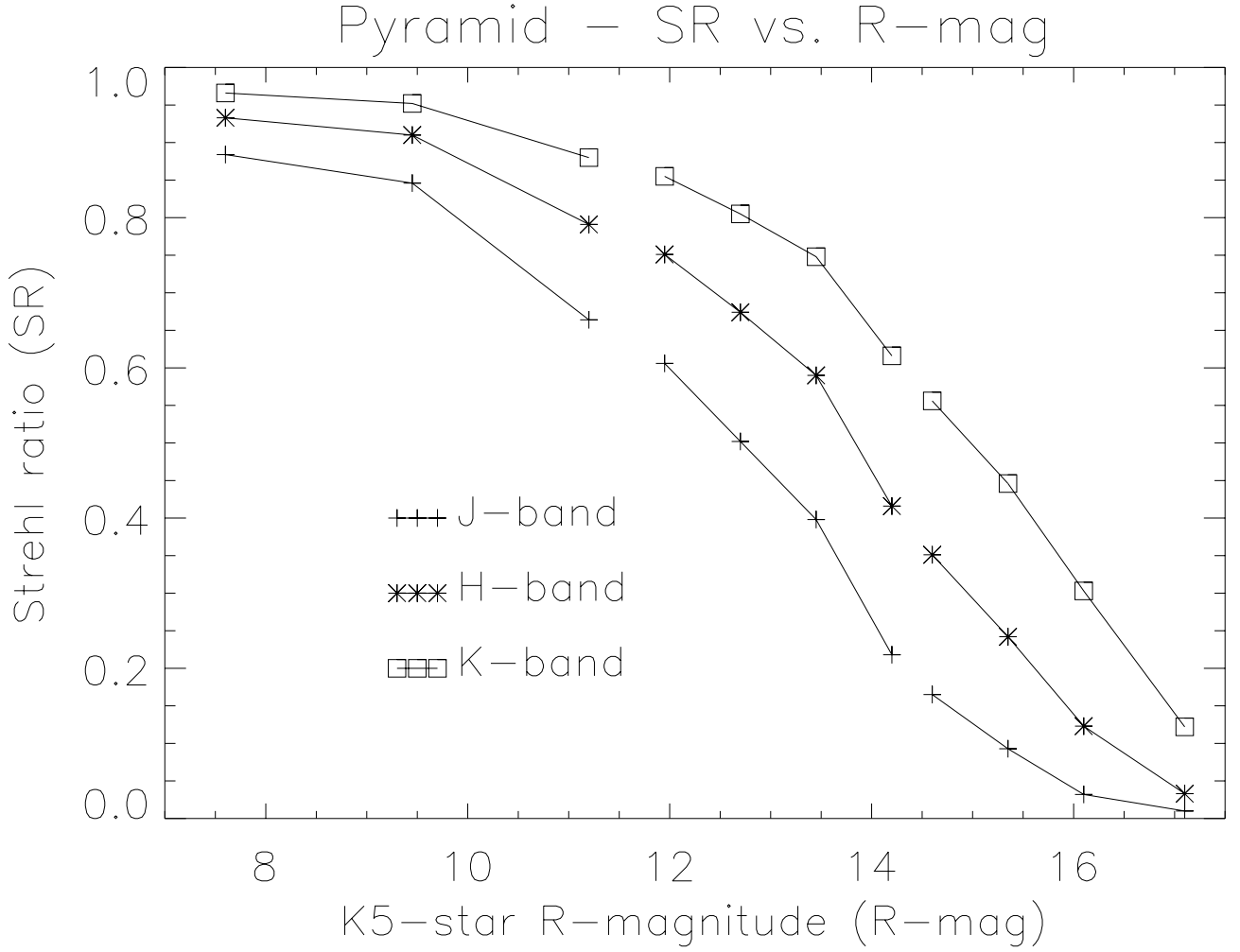
4.1. Pyramid vs. Shack-Hartmann

Figure 5 shows the comparison with a Shack-Hartmann-based equivalent system in terms of K-band Strehl ratios. The plot clearly shows the expected gain of the pyramid in terms of limiting magnitude,^{6,11} in close-loop operation and including the residuals from the atmospheric uncorrected modes. The gain around R-mag=16 is roughly of 1 mag., leading to a gain in sky coverage shown as described hereafter. We are also investigating the small gain at high-Strehl regime that could be due to a difference in the propagation of aliasing noise.

4.2. Sky coverage

By using the Bahcall & Soneira model of distribution of stars¹ we can evaluate the sky coverage achievable when a given Strehl ratio is desired. An important additional parameter to take into account is at this point is the maximum correction angle considered. Let us note it θ_{\max} and take for it 30 arcsec in K-band. The corresponding area of sky is then $\pi\theta_{\max}^2$, and the sky coverage is then $1 - \exp\{-\mathcal{N}\}$, where \mathcal{N} is the number of stars of a given R-magnitude in that area. Let us also consider a minimum Strehl ratio of 20%, that would decrease of roughly 10% at 30 arcsec from the guide star. This value of Strehl corresponds to an R-mag. of ~ 16.65 for the pyramid and ~ 15.54 for the Shack-Hartmann, as deduced from Fig. 4 and Fig. 5.

By reporting these values on the sky coverage vs. R-mag. plot, one can easily deduce that for a median case ($b=20, l=180$) the sky coverage passes from $\sim 18\%$ for the SH to $\sim 33\%$ for the PS. For the two other cases the sky coverage passes from $\sim 6\%$ to $\sim 11\%$ and from $\sim 47\%$ to $\sim 82\%$, for a pessimistic case ($b=90$) and a more optimistic case ($b=20, l=0$), respectively.



K5 star R-mag.	config.	Δt [ms]	\Rightarrow RON [e ⁻ rms]	n_M	pyr. mod. [λ/D]	S_J (PS)	S_H (PS)	S_K (PS)
7.60	30×30	1.00	\Rightarrow 8.4	671	± 1	.884	.933	.966
9.45	30×30	1.00	\Rightarrow 8.4	496	± 2	.846	.910	.952
11.20	30×30	1.67	\Rightarrow 8.4	496	± 2	.664	.791	.880
11.95	15×15	1.67	\Rightarrow 5.8	136	± 3	.606	.751	.855
12.70	15×15	1.67	\Rightarrow 5.8	136	± 3	.502	.674	.805
13.45	15×15	2.50	\Rightarrow 4.5	136	± 3	.398	.590	.748
14.20	15×15	2.50	\Rightarrow 4.5	105	± 3	.218	.416	.616
14.60	10×10	2.50	\Rightarrow 4.5	66	± 4	.165	.351	.556
15.35	10×10	5.00	\Rightarrow 3.5	55	± 4	.093	.242	.446
16.10	10×10	5.00	\Rightarrow 3.5	55	± 5	.032	.123	.303
17.10	10×10	10.00	\Rightarrow 3.5	45	± 6	.010	.033	.122

Figure 4. First-light LBT AO system performance (in terms of J-, H-, and K-band Strehl ratios) versus the guide star R-magnitude, and corresponding main parameters of the simulation.

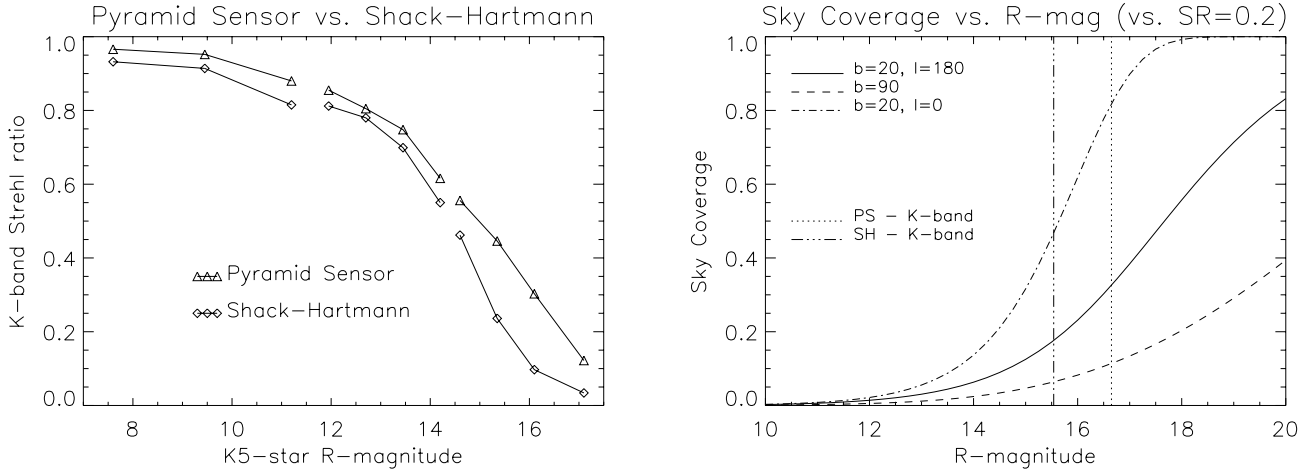


Figure 5. Comparison with a Shack-Hartmann-based equivalent system in terms of K-band Strehl ratio [left] and subsequent sky coverage, for different regions of the sky [right].

5. CONCLUSIONS

By analysing the previous exposed results, and even if a number of additional tests are being performed in order to explore even more deeply the hyperspace of parameters, we can already reach to some simple conclusions, and namely:

1. when the number of photons per time unit is high (and up to the 11th magnitude), the use of the 30×30 configuration with a relatively high number of modes corrected (496–671), a short integration time (1–1.67 ms), and a small modulation of the pyramid ($1-2\lambda/D$), allow to reach very high performance in terms of Strehl ratio ($\sim 90\%$ in K for a R-magnitude of ~ 10).
2. then the use of the 15×15 configuration, still with a relatively high number of corrected modes (105–136) but with a larger integration time (up to 2.5 ms), becomes more convenient (from around the 12th magnitude), mainly due to the fact that the RON tends to be more and more an issue.
3. the regime with less photons (after the magnitude ~ 14.5) benefits from using the 10×10 configuration, with an increasing integration time (from 2.5 ms at magnitude 14.6 to 10 ms at magnitude 17.1), an increasing pyramid modulation (from $4\lambda/D$ to $6\lambda/D$), and a decreasing number of corrected modes (from the relatively high 66 number of modes down to the more modest 45 number of modes).
4. the gain of using the pyramid sensor with respect to the Shack-Hartmann one is clearly shown, especially for the faintest stars for which the resulting gain in sky coverage is also shown.

5.1. A couple of additional remarks...

In addition to consider the use of the deep depletion CCD, we consider here also the L3CCD that permits very low RON.¹⁰ Figure 6 shows the gain that would be obtained with a RON of $0.5 e^-$ rms (instead of 3.5–4.5 for the deep depletion CCD): roughly 1 more magnitude for a Strehl ratio in K-band of ~ 0.3 .

Another interesting point is about the pyramid modulation during recording of the interaction matrix *and* during correction. The simulations presented here were done by applying the same modulation during both. We are investigating the best strategy for using modulation, taking into account the effect of “natural” modulation due to the residuals at the sensing wavelength. See the dedicated paper by Buechler Costa et al.⁵ for more information.

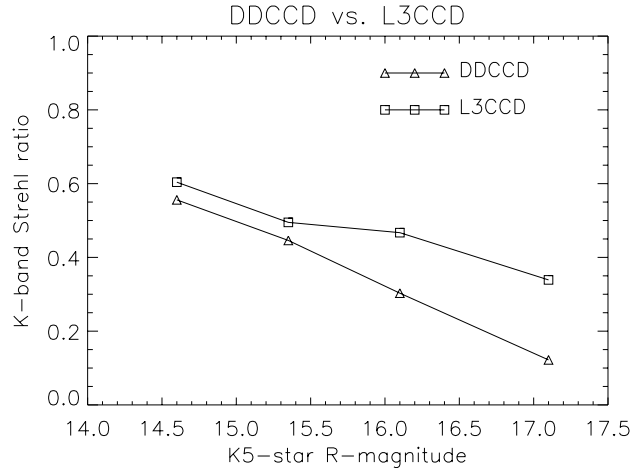


Figure 6. Deep depletion CCD vs. L3CCD.

REFERENCES

1. J. N. Bahcall & R. M. Soneira, *ApJ Supp. Ser.* **44**, pp. 73–110, 1980.
2. M. Carbillet, L. Fini, B. Femenía, A. Riccardi, S. Esposito, É. Viard, F. Delplancke, N. Hubin, in *ASP Conf. Series* **238**, F. A. Primini & F. R. Harnden Eds, pp. 249–252, 2001.
3. S. Correia, M. Carbillet, L. Fini, P. Boccacci, M. Bertero, A. Vallenari, A. Richichi, M. Barbati, in *ASP Conf. Series* **238**, F. A. Primini & F. R. Harnden Eds, pp. 404–407, 2001.
4. S. Correia, M. Carbillet, P. Boccacci, M. Bertero, L. Fini, *Astron. Astrophys.* **387**, pp. 733–743, 2002.
5. J. Buechler Costa, R. Ragazzoni, A. Ghedina, M. Carbillet, C. Vérinaud, M. Feldt, S. Esposito, S. Hippler, J. Farinato, Proc. SPIE 4839, P. L. Winizowitch & D. Bonaccini Eds, to be published, 2002.
6. S. Esposito & A. Riccardi, *Astron. Astrophys.* **369**, pp. L9–L12, 2001.
7. S. Esposito, A. Tozzi, D. Feruzzi, M. Carbillet, A. Riccardi, L. Fini, C. Vérinaud, M. Accardo, G. Brusa, D. Gallieni, R. Biasi, C. Baffa, V. Billiotti, I. Foppiani, A. Puglisi, R. Ragazzoni, P. Ranfagni, P. Stefanini, P. Salinari, W. Seifert, J. Storm, Proc. SPIE 4839, P. L. Winizowitch & D. Bonaccini Eds, to be published, 2002.
8. L. Fini, M. Carbillet, A. Riccardi, in *ASP Conf. Series* **238**, F. A. Primini & F. R. Harnden Eds, pp. 253–256, 2001.
9. J. Hill & P. Salinari, Proc. SPIE 4837, J. M. Oschmann & L. M. Stepp Eds, to be published, 2002.
10. I. Foppiani, C. Baffa, V. Billiotti, G. Bregoli, G. Cosentino, E. Giani, S. Esposito, B. Marano, P. Salinari, Proc. SPIE 4837, J. M. Oschmann & L. M. Stepp Eds, to be published, 2002.
11. R. Ragazzoni & J. Farinato, *Astron. Astrophys.* **350**, pp. L23–L26, 1999.
12. A. Riccardi, G. Brusa, P. Salinari, D. Gallieni, R. Biasi, M. Andrighettoni, H. M. Martin, Proc. SPIE 4839, P. L. Winizowitch & D. Bonaccini Eds, to be published, 2002.
13. J. Storm, W. Seifert, S. Bauer, F. Dionies, U. Hanschur, J. Hill, G. Moestl, P. Salinari, W. Varava, H. Zinnecker, Proc. SPIE 4839, P. L. Winizowitch & D. Bonaccini Eds, to be published, 2002.
14. C. Vérinaud, M. Carbillet, B. Femenía, SF2A 2002, EDP-Sciences Conf. Series, F. Combes & D. Barret Eds, in press, 2002.
15. C. Vérinaud, C. Arcidiacono, M. Carbillet, E. Diolaiti, R. Ragazzoni, É. Vernet-Viard, S. Esposito, Proc. SPIE 4839, P. L. Winizowitch & D. Bonaccini Eds, to be published, 2002.